How to Model Solvent Effects on Molecular Properties Using Quantum Chemistry? Insights from Polarizable Discrete or Continuum Solvation Models

Jacob Kongsted*

Department of Theoretical Chemistry, Chemical Center, University of Lund, P.O. Box 124, S-221 00 Lund, Sweden

Benedetta Mennucci

Department of Chemistry, University of Pisa, Via Risorgimento 35, 56126 Pisa, Italy

Received: June 5, 2007; In Final Form: July 27, 2007

We present a comparative study of solvent effects on the ^{15}N NMR shielding constants and the lowest electronic excitation energy (n → π^*) in the three diazines (pyrazine, pyrimidine, and pyridazine) in aqueous solution. This solvent is modeled using either a polarizable continuum model (PCM) or a discrete polarizable model (DPM). We analyze the results obtained with the two models in terms of differences/similarities in the reaction field produced at the solute. The PCM reaction field is found to be quite sensitive to the dimension of the cavity and so are the molecular properties. However, constructing the cavity so that the DPM and PCM reaction fields become similar in magnitude leads to quite similar results for the studied molecular properties modeling the solvent using either the PCM or the DPM. Compared to experimental data, the most accurate predicted results are obtained by describing the closest water molecules at the same level of sophistication as that of the solute, whereas the bulk solvent may be described using either PCM or MM. Finally, a comparison with geometry-optimized clusters seems to show that it is important to check potential deficiencies in the force field in order for this to treat hydrogen bonding in a consistent manner.

I. Introduction

A long-standing problem in theoretical chemistry concerns development and benchmarking of solvation models. Even though quantum chemistry for small isolated molecules has reached the limit of chemical accuracy,[1] the same cannot be said for molecules subjected to an environment, for example, a solute in a solvent. The difficulties one encounters by introducing an environment are manifold. First of all, the size of the system will naturally exceed that of the isolated system, and due to the long-range nature of some of the intermolecular forces, this increase may be quite drastic. Consider, for example, the case of a small organic solute in a water solution under standard conditions. Defining a cutoff for the electrostatic interaction at 12 Å will amount to considering around 240 explicit water molecules in addition to the solute. Second, the solvent is, by nature, inherently dynamical, meaning that configurational sampling is mandatory. Effective approaches have been developed in order to reduce the number of solute−solvent configurations needed in order to arrive at converged results,[2] but usually at least 100 configurations must be used. In some cases and for some molecular properties, this number may however be a factor of ∼8−10 higher.[3] Finally, in contrast to the case of an isolated molecule, symmetry is usually not present in large solute−solvent samples, which increases the computational requirements further. From this example, it is evident that even though linear scaling methods have become quite efficient also for the evaluation of general molecular properties[4] and outstanding progress in parallelization and development of highly flexible computer platforms has been made, a brute force method for introducing solvent effects still represents an enormous increase in computational time as compared to the corresponding calculation for an isolated molecule. It is thereby not only instructive but also in many cases necessary to introduce approximations in the way the solvent is described. One approach is of course to neglect the contribution from the most distinct solvent molecules, for example, to use a truncated cluster approach to model solvation. Such a procedure has been widely used in the literature due to the fact that the atomistic nature of the nearby solvent molecules are kept. However, the contribution from the bulk solvent cannot generally be neglected, and such a procedure is therefore not recommended. Rather, one should, in our opinion, construct solutions to the problem where the solvent, or at least the major part of it, should be treated effectively, that is, by use of an effective Hamiltonian where only a part of the total system is treated explicitly. This, in fact, is the main idea in the successful introduction of effective core potentials for heavy atoms where the core electrons are described by a potential that acts on the valence electrons.

Effective solvent models may generally be divided into two main categories, (i) the dielectric continuum (DC) models and (ii) the discrete solvation models. In the first approach, the solvent is modeled as a macroscopic dielectric continuum characterized by a dielectric constant. Thus, any reference to the atomistic nature of the solvent is neglected, and configurational sampling is included implicitly. Thus, for this model, no explicit simulations have to be conducted, and no explicit sampling is necessary. The possible disadvantages are, however, that the DC model completely neglects the local anisotropies

* To whom correspondence should be addressed. E-mail: Jacob.Kongsted@ teokem.lu.se.

10.1021/jp074343w CCC: $37.00
Published on Web 09/11/2007

CHART 1

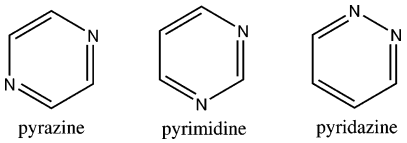

around the solute, which only, on average, will tend to zero, caused by the discrete solvent molecules. A more technical but still relevant problem with the DC model is the definition of the cavity which contains the solute inside of the dielectric medium. The surface of such a cavity represents the physical boundary between the solute and solvent, and thus, its shape and dimension becomes of fundamental importance in the description of their interactions. Nowadays, cavities used in the most accurate DC models can account for the real 3D structure of the solute being defined in terms of interlocking spheres centered on the solute nuclei.[5] However, there still remains the uncertainty of which radii are to be used; too small values, in fact, could lead to nonphysical interactions, while too large values will result in a too small interaction and thereby to a significant underestimation of the solvent effects on specific molecular properties. Furthermore, when properties and/or phenomena involving excited states are under scrutiny, we also have to take into account that these states are usually more diffuse than the ground state, and choosing a reasonable cavity size for the latter states may lead to potential artifacts concerning the solvation of the excited states.

In the second approach, the reference to a discrete solvent is kept. In order for the latter approach to be effective, the solvent, or at least the major part of this, may be treated classically. This leads to the definition of the combined quantum mechanics/molecular mechanics (QM/MM) approach.[6−9] In the simpler versions of this approach, the solvent is treated simply by assigning partial point charges to the atomic sites, and the potential due to these point charges is then introduced into the solute Hamiltonian. However, in such a procedure, polarization of the solvent is neglected, that is, only the solute is polarized. This may be refined, for example, by assigning polarizable sites to the solvent giving rise to induced electrical moments. The mutual solute−solvent scheme requires an iterative solution of the Schrödinger equation. In the dielectric continuum model, the solvent is also polarized by the solvent, meaning that comparison between the performance of the DC and QM/MM models should be performed using a polarizable QM/MM scheme.

The completely different characteristics of the DC and discrete solvation models make it interesting to compare their performances when describing the effects of the solvent on molecular response properties; these, in fact, are known to be much more sensitive to the quality of the model used with respect to solvation energies. A very good candidate for such a comparative analysis is the NMR shielding constant. This property, in fact, is very sensitive to the chemical environment, and especially, hydrogen bonding may change the magnitude of the resonance frequencies. An alternative, and in some way complementary, source of specific information about solute−solvent interactions is the UV spectroscopy. Both NMR and UV spectroscopic properties are studied in this paper in which we will present an analysis of environmental effects on the three diazines, that is, pyrazine, pyrimidine, and pyridazine (see chart). All of these three compounds contain two sp^2-type nitrogens and are thus capable of performing hydrogen bonding to a protic solvent. In the present context, we will consider water as the solvent. Our aim is to compare the polarizable continuum model (PCM) (see ref 5 for a recent review) with the discrete polarizable model (DPM), which we have recently derived and implemented at the coupled-cluster (CC),[10] density functional theory (DFT),[11] or Hartree−Fock (HF)[11] level of theory. Here, only the DFT level will be exploited using the B3LYP[12] exchange-correlation functional. Since both of these solvent models include solvent polarization, their performance can be compared directly. This means that the intrinsic approximations in the PCM model, for example, implicit averaging and neglect of specific interactions, can be explored. The diazines have been chosen since these compounds have been studied for a long time from both an experimental[13−15] and theoretical point of view.[16−20] In addition, a large spread in the solvent shifts on the NMR shielding constants and UV properties are found within the diazines, which can be used further to test the performance of the solvation models.

This paper is organized as follows. In section II, we present the two different solvent models in more detail. Section III contains the computational details, and in section IV, we present and discuss the results. Finally, a summary ends this paper.

II. Method

As reported in the Introduction, we compare in the present work two different approaches (PCM and DPM) for introducing the effect of a solvent on a solute. Below, we discuss shortly the physics and methodological handling of the two solvent models employed.

A. The Polarizable Continuum Model. Within the PCM, the solvent is represented as a homogeneous dielectric continuum which is polarized by the solute placed in a molecular-shaped cavity. The latter is obtained by assigning a sphere of given radius to each atom (or a group of atoms) forming the solute and considering the final envelope of these interlocking spheres. A cavity scaling factor (f) is usually introduced to enlarge the basic atomic or group radii before the individual spheres are defined.[21] The general strategy is then to solve the Poisson equation (with appropriate boundary conditions), which univocally defines the potential characterizing the electrostatics of this problem. This may be done using different mathematical approaches. In particular, we will apply the integral equation formalism (IEF)[22] version of PCM, which makes use of operator functions derived from the theory of integral equations. Within this approach, the potential is given as a sum of the potential produced by the solute charge distribution and the potential due to an apparent surface charge (ASC) distribution which arises due to polarization of the dielectric medium. The latter charge distribution gives rise to the reaction field acting back on the solute. In order to solve for the ASC distribution, a partitioning of the cavity surface into N finite elements, called tesserae, is performed. Each portion of the surface then carries a point charge (q_k). Within this picture, the potential due to the polarization of the dielectric medium may be written as a discrete sum

$$\phi(\mathbf{r}) = \sum_{k=1}^{N} \frac{q_k}{|\mathbf{r} - \mathbf{r}_k|} \tag{1}$$

where $\mathbf{r}_k$ is the position of tesserae k. The point charges entering eq 1 may be determined from a matrix equation

$$\mathbf{q} = -\mathbf{K}(\epsilon)\mathbf{V} \tag{2}$$

where the vector $\mathbf{V}$ collects the solute electrostatic potential at the tesserae. Furthermore, $\mathbf{K}$ is a square matrix (the dimension

being equal to the number of tesserae), which depends on the geometrical cavity parameters and the dielectric constant of the solvent (see ref 5 for more details).

The coupling between the solute and the PCM is introduced by adding to the Hamiltonian of the isolated molecule ($\hat{H}_0$) the electrostatic potential in eq 1, that is, we define the following effective Hamiltonian

$$\hat{H}_{\text{eff}}|\Psi\rangle = (\hat{H}_0 + \hat{\phi})|\Psi\rangle = E|\Psi\rangle \tag{3}$$

where we have introduced an electronic operator $\hat{\phi}$ corresponding to the electrostatic potential in eq 1. Note that the potential depends on the electronic density through eq 2, which means that eq 3 becomes nonlinear in Ψ. For this specific case, solving eq 3 is equivalent to minimizing the following free-energy functional

$$G(\Psi) = \langle\Psi|\hat{G}|\Psi\rangle = \left\langle\Psi\left|\hat{H}_0 + \frac{1}{2}\hat{\phi}\right|\Psi\right\rangle \tag{4}$$

Minimization of eq 4 with respect to the electronic wave function parameters will, in the case of a self-consistent-field (SCF) method, lead to the specific expression for the effective Fock/Kohn−Sham operator.

B. The Discrete Polarizable Model. The main difference between the PCM and the discrete polarizable model (DPM) is that the latter keeps the reference to the atomistic nature of the solvent molecules. Thus, one considers here either a mean structure representing the solute in the discrete solvent or a collection of solute−solvent structures usually obtained from molecular dynamics (MD) or Monte Carlo (MC) simulations. The permanent charge distribution of the solvent molecules is represented through multicenter multipole expansions. In the present work, we truncate this expansion after the charge term. In addition, molecular dipole polarizabilities are assigned to each solvent molecule. The use of distributed polarizabilities is straightforward. However, for small solvent molecules with low anisotropies in the molecular polarizability, the use of monocenter polarizabilities is usually sufficient. In order to account effectively for short-range repulsion and dispersion, a set of Lennard-Jones parameters is assigned to each solvent molecule. We emphasize that the way the polarizable force field is constructed is physically well-motivated. The partial charges are chosen such as to reproduce the molecular dipole moment of the gas-phase molecule, and the introduction of the polarizability leads, in the condensed phase, to the well-known increase of the dipole moment and furthermore keeps a reference to a true fluctuating dipole moment for each solvent molecule.

Within the DPM, the solute and solvent are mutually polarized self-consistently. The polarizabilities of the solvent molecules give rise to microscopic-induced dipole moments ($\boldsymbol{\mu}_a^{\text{ind}}$) at the polarizable sites (a) in the solvent. These are determined using an equation of the form

$$\boldsymbol{\mu}_a^{\text{ind}} = \boldsymbol{\alpha}_a(\mathbf{E}_a^{\text{solute}} + \mathbf{E}_a^{\text{solvent}}\{\boldsymbol{\mu}^{\text{ind}}\}) \tag{5}$$

In eq 5, $\mathbf{E}_a^{\text{solute}}$ ($\mathbf{E}_a^{\text{solvent}}$) is the electric field calculated at site a due to the solute (solvent). As indicated in eq 5, the electric field at site a from the solvent (and hence the induced dipole at that site) depends on all other induced dipole moments in the solvent. This means that eq 5 must be solved iteratively within each SCF iteration. As an alternative, eq 5 may, in a dipole approximation, be restructured into a matrix equation

$$\boldsymbol{\mu}^{\text{ind}} = \mathbf{BE} \tag{6}$$

The matrix $\mathbf{B}$ is of dimension $3N\otimes 3N$, where N is the number of polarizable sites, and the vector $\mathbf{E}$ collects the electric field from the solute and the solvent permanent charge distribution.

In case of the DPM, the expression for the coupling between the solute and the solvent is derived along the same lines as that in case of the PCM, that is, an effective operator is constructed and added to the Hamiltonian for the isolated molecule.[10,11,23] In the case of the DPM, this operator contains a contribution due to the multipole distribution of the permanent charge distribution of the solvent molecules and a term related to the polarization (induced multipole moments) in the solvent. In addition, nonelectrostatic solute−solvent interactions may be included.

C. Evaluation of Molecular Properties. In the preceding sections, we have described the basics of the PCM and the DPM for introducing solvent effects in quantum chemical calculations. In both cases, an appropriate interaction operator between the solute and solvent is added to the Hamiltonian of the isolated molecule. The interaction is described by a one-electron operator, and no significant increase in computational effort is introduced. The electronic density is obtained by including self-consistently the polarization of the solvent. Along the same lines as that for an isolated molecule, the use of response theory may, in the context of solvation, be used to study a variety of molecular properties other than the molecular energy. Introducing the concepts of response theory into the PCM or DPM partitioning leads to a compact and powerful method to calculate general frequency-dependent molecular properties of a molecule subjected to an environment. In particular, both properties related to external or internal perturbations may be considered. In addition to this, the specific properties may be of either electric or magnetic origin. Specific details concerning theoretical and implementation aspects of DFT/PCM or DFT/MM in the context of response theory may be found in refs 5 and 11, respectively.

In the present context, we will exclusively discuss the linear response function[24] since this will provide us with the tools for calculating vertical electronic excitation energies and absorption properties (UV spectra) and also will allow us to consider NMR shielding tensors. It is advantageous to use response theory for the calculation of general-order molecular properties since, in this approach, the molecular properties are evaluated by solving response equations rather than considering the computationally inconvenient sum-over-states expressions. In particular, response theory allows for calculation of transition properties without explicit reference to the excited states.

Within the DPM, the specific contributions due to the polarizable and structured environment will lead to two different sorts of corrections,[11] (i) contributions due to the static multipole moments (here partial charges) and (ii) contributions due to the induced polarization in the environment as a consequence of the time-dependent perturbation. In contrast, for the PCM, only contributions due to the induced polarization in the solvent are relevant.[25] Having obtained the linear response function, it is well-known that electronic excitation energies and absorption properties may be obtained from the poles and residues, respectively.[26]

The response functions as outlined above may, in principle, be applied directly to the calculation of properties of both electric and magnetic origin. However, for magnetic and mixed electric−magnetic properties, it is well-known that the vector potential included in the electronic Hamiltonian contains a reference to the global gauge origin. Thereby, in approximate theory, the calculated magnetic properties will generally depend on the global gauge origin and, in this way, introduce an origin

dependence in the calculated magnetic properties.[27] In order to ensure origin-independent results for the nuclear magnetic shielding constants, we use gauge-including atomic orbitals (GIAOs),[28,29] that is, the atomic orbital basis functions depend explicitly on the magnetic induction. Using GIAOs, specific corrections due to the effective operator describing the environment will arise in the response equations corresponding to the perturbation from the magnetic induction. The detailed derivation of such corrections have been considered in refs 30 and 31 for the PCM model and in ref 32 for the DPM within either a HF or DFT description of the solute molecule.

III. Computational Details

In this section, we describe the computational details. First, we consider the MD simulations and next, the electronic structure calculations.

A. MD Simulations. In order to generate an appropriate number of solute−solvent configurations to be used in the UV and NMR calculations, a series of classical MD simulations of pyrazine, pyrimidine, or pyridazine in aqueous solution has been carried out using the Molsim program package.[33] The force fields for the diazines have been taken from ref 34 using reoptimized molecular geometries at the B3LYP/aug-cc-pVTZ/PCM level of theory. The geometry optimizations have been performed using the PCM model as implemented in the Gaussian 03 program.[35] For water, the polarizable SPCpol potential of Ahlström et al.[36] has been used together with the intramolecular geometry of water of $R_{OH} = 0.9572$ Å and $\angle_{HOH} = 104.49°$. The use of a polarizable force field leads to the introduction of many-body effects in the MD simulation and thereby to cooperativity in the hydrogen-bonding network.

The MD simulations were performed in a cubic box within the NVT ensemble at the temperature of 298.15 K. We considered 1 rigid solute and 511 rigid water molecules. The box side was fixed to 24.91 Å in order to reproduce the experimental density of liquid water. We employed periodic boundary conditions together with a spherical cutoff distance for the electrostatic interactions at half of the box length. To account for the long-range and polarization interactions, a reaction-field correction was considered. The induced dipole moments were recalculated every third time step with a relative tolerance of 10^{-7}. The initial equilibration was carried out for 300 ps with a time step of 2 fs, followed by the production run of 600 ps. The configurations were dumped every 1 ps, and we thus obtained 600 molecular configurations to use in the subsequent electronic structure calculations.

B. Electronic Structure Calculations. The 600 solute−solvent configurations derived from the MD simulations were next introduced into electronic structure calculations. Each configuration was translated/rotated so that the solute molecule adopted a reference geometry. Next, a spherical cutoff distance was applied to every molecular configuration extracted from the MD simulation. On the basis of test calculations, this cutoff radius was set equal to 12 Å. This cutoff distance includes ∼230−240 water molecules together with the solute. In the DPM calculations, the solute and potentially a number of the closest water molecules were the treated using DFT/B3LYP, while the rest of the solvent was treated classically using the same polarizable potential as that in the MD simulations. Acronyms like DFT(*X*)/MM indicate a DFT/MM calculation where *X* water molecules have been included into the part of the system treated using DFT. For the PCM calculations, only the two closest water molecules, with respect to each of the nitrogen atoms in the solute, were kept within the molecular complex, and the effect of the rest of the solvent was then treated using the PCM. In addition, we also performed calculations where all of the explicit solvent molecules were replaced by the PCM. A molecular property in solution was evaluated as a statistical average over all molecular configurations, and finally, the gas-to-aqueous solution shift of the molecular property was determined as the difference with respect to the corresponding reference in vacuum.

The DFT/MM calculations have been performed using the development version of the Dalton quantum chemistry program.[37] The DFT/PCM calculations have been performed using the Gaussian 03 program;[35] the cavities of all of the diazines has been obtained using a united atom approach in which hydrogen atoms are inside of the sphere centered on the linked carbon atom (the radii used are 1.77 Å for CH and 1.53 Å for N, while the scaling factor has been varied from 1.1. to 1.4). The statistical analysis have been done using the MidasCpp[38] program. In all geometry optimizations, we have used the aug-cc-pVTZ basis set,[39] and in all property calculations, we have used the 6-311++G(2d,2p) basis set,[40] which has previously been shown to give very accurate results for nuclear chemical shielding constants.[41,42] This basis set is also of modest size and therefore allowed us to perform calculations where also some of the solvent molecules are described using DFT.

In all calculations, we neglected rovibrational averaging. Differential rovibrational effects may, however, be important for accurate evaluation of the gas-to-aqueous solution shifts of NMR shielding constants, and therefore, they represent a potential source of uncertainty in our work.

IV. Results and Discussion

A. MD Simulations. In Figure 1, we show the radial distribution functions (RDFs) between one of the nitrogen atoms of pyrazine (a), pyrimidine (b), or pyridazine (c) and the water hydrogen derived from the SPCpol MD simulation.

The first maximum in each of these RDFs indicates the length of the hydrogen bond, which amounts to 2.07 Å for pyrazine, 1.96 Å for pyrimidine, and 2.16 Å for pyridazine. These hydrogen bond lengths are roughly proportional to the effective charge assigned to the nitrogen sites (−0.468, −0.839, and −0.331, respectively). The hydrogen coordination number to the nitrogen site is almost constant and is, by spherical integration of the RDFs, found to be around 1.0 for pyrazine, 1.2 for pyrimidine, and 1.4 for pyridazine. Since each diazine contains two nitrogen sites, the hydrogen coordination number for each solute is found by multiplying the respective nitrogen coordination numbers by a factor of 2. We note that these numbers represent an upper limit for the number of water molecules hydrogen bonded to the solutes. This is due to the fact that we have not considered any additional constraints such as geometric and/or energetic criteria for defining a hydrogen bond (see, for example, the detailed study in ref 43). In the electronic structure calculations based on the derived solute−solvent configurations from the MD simulations, a number of explicitly treated water molecules may be introduced into the region treated using quantum mechanics. In this respect, we will always treat the two nitrogen atoms in the solutes as equivalent, including, for example, two explicit water molecules means that either nitrogen atom coordinates one water molecule (as indicated in Figure 5).

B. Convergence Analysis. An important subject is to consider the convergence of the calculated properties with respect to the number of solute−solvent configurations included in the statistical procedure in order to obtain converged results. Canuto and

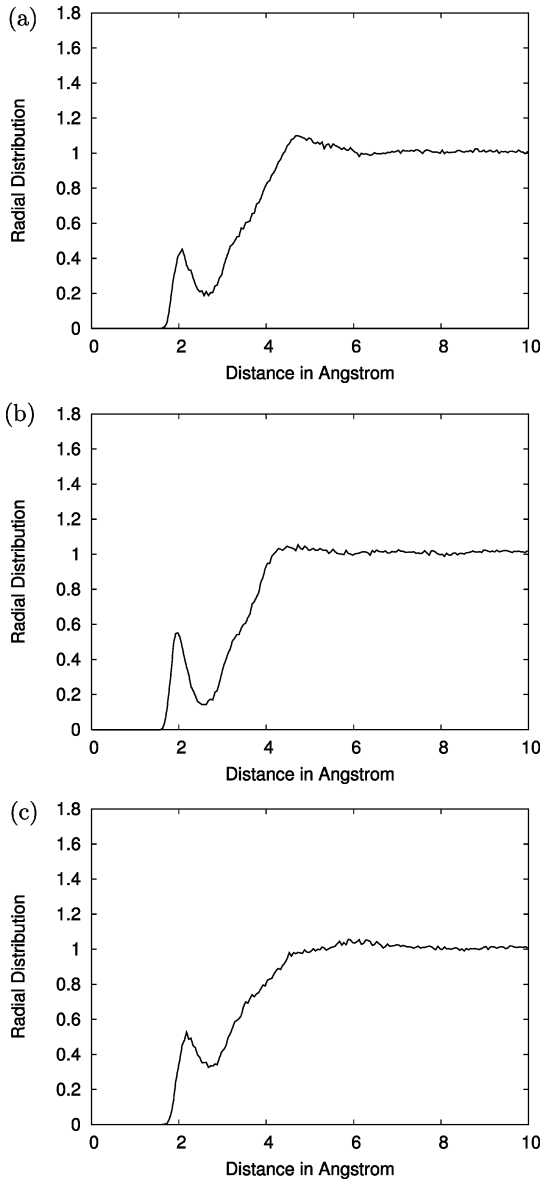

Figure 1. The H(water)−N(diazine) radial distribution function obtained from the MD simulation; (a) pyrazine, (b) pyrimidine, and (c) pyridazine.

co-workers have extensively made use of the autocorrelation function of the energy in order to extract uncorrelated solute−solvent configurations to be used in combined quantum mechanics/molecular mechanics calculations.[2] The minimum number of solute−solvent configurations to be included in the statistical analysis may however depend on the nature of the molecular property in question. In Figure 2, we show (a) the lowest electronic excitation energy and (b) the isotropic nitrogen shielding constant as function of the number of configurations included in the averaging.

The solute is pyrimidine. The calculations have been performed using the DPM model with only the solute treated using quantum mechanics. As seen from Figure 2, both the electronic excitation energy and the NMR shielding constant appear to be converged based on around 100 configurations. In the following, we have chosen to use 200 configurations in the statistical averaging since this number of configurations clearly provides statistically converged molecular properties. Also, the effect of using a larger number of configurations is to obtain a smaller statistical error in the mean values.

C. The Lowest n → π* Electronic Excitation Energy. We begin by discussing the results for the solvent effect on the lowest electronic excitation energy, which is of n → π^* character and is found to be located well below the lowest electronic excitation energy in the solvent (water). Furthermore, this excitation is expected to be rather localized within the solute fragment. In the electronic ground state, each of the diazines is in a polar solvent stabilized through hydrogen bonding involving the lone pair on the nitrogen atoms. In the n → π^* state, however, this stabilizing effect is reduced, and thereby, a blue shift of this electronic excitation is expected. The differential amount of the blue shift within the diazines is largely dependent on the ground-state electronic dipole moment. The dipole moment increases for the molecules listed in Table 1 and in Figure 3 going from left to right and so does the blue shift, according to experimental observations.

Considering first the "bare" PCM with the standard cavity (i.e., scaling factor of $f = 1.2$) in which only the solute is treated using quantum mechanics and all solvent molecules are replaced by a dielectric, we observe that the trends in the experimental data are reproduced, but the magnitude of the shifts are clearly underestimated and, in some cases, quite largely. Thereby, it seems that the above discussion concerning explicit hydrogen bonding is very important in the present case.

The effect of explicit hydrogen bonding may be accounted for in different ways. We can either rigorously consider the first-shell water molecules in an explicit way, or we can use an effective cavity, which, by artificially increasing the solute−solvent bulk interactions, can simulate the additional effect of the hydrogen bonds. This effective cavity is easily obtained by decreasing the scaling factor f but still satisfying the fundamental request of having a physically meaningful cavity; a reasonable value is $f = 1.1$. As shown in Table 1, this leads to a general increase in the excitation energies (except for pyrazine, where the value is unchanged) and thereby to an improved comparison with the experimental data; see Figure 3.

As discussed previously, a more rigorous solution is to consider some of the water molecules explicitly. In a first approximation, a limited number of explicit water molecules may be introduced. In the DFT(2) results included in Table 1 and in Figure 3, a statistical averaging has been performed over the 200 MD-derived configurations, but only the two water molecules closest to the nitrogen sites have been considered, that is, the outer-shell solvent molecules have been neglected. The two closest water molecules have, in turn, been treated at the same electronic structure level as that of the solute. As seen from Figure 3, such an approach leads to largely underestimated blue shifts. This clearly indicates that it is not enough to consider only specific effects but that the coupling to the bulk solvent plays an extremely important role.

This can be shown and quantified by combining specific and bulk effects together with statistical averaging; these are the DFT(2)/PCM results. Here, the two water molecules closest to the nitrogen sites of the solute are treated using DFT, while the rest of the solvent is modeled as a PCM dielectric. This approach is very much in line with previous work by Karelson and Zerner[17] on early calculations on solvent effects on electronic excitation energies for pyrimidine in water solution. On the basis of small solute−solvent clusters embedded into a dielectric continuum, the authors concluded that both specific hydrogen bonding and bulk effects were important to correctly reproduce the experimental observations. In our case, on the basis of statistical averaging, compared to the DFT(2) results, improvements are generally found in a very similar way as what were

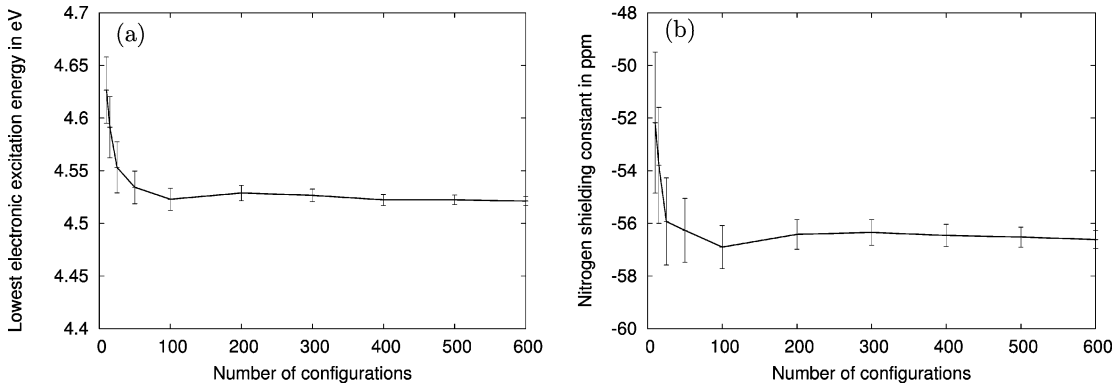

Figure 2. Convergence of (a) the lowest electronic excitation energy and (b) the nitrogen shielding constant of pyrimidine in aqueous solution. The calculations have been performed using B3LYP/6-311++G(2d,2p).

TABLE 1: The Lowest Electronic Excitation Energy in the Three Diazines in Vacuum and in Aqueous Solution[a]

method	pyrazine	pyrimidine	pyridazine
vacuum	3.95	4.28	3.55
DFT/PCM ($f = 1.2$)	4.00	4.45	3.89
DFT/PCM ($f = 1.1$)	4.00	4.49	3.95
DFT(2)	3.95 ± 0.01	4.30 ± 0.01	3.65 ± 0.01
DFT(2)/PCM	4.00 ± 0.01	4.48 ± 0.01	3.92 ± 0.01
DFT/MM	4.05 ± 0.01	4.52 ± 0.01	3.85 ± 0.01
DFT(2)/MM	4.03 ± 0.01	4.49 ± 0.01	4.03 ± 0.01
DFT(4)/MM		4.48 ± 0.01	

[a] The calculations have been performed using B3LYP/6-311++G(2d,2p), employing preoptimized geometries of the diazines computed at the B3LYP/aug-cc-pVTZ(/PCM) level of theory. The water potential used in the QM/MM calculations is the SPCpol. The number of solute−solvent configurations included in the averaging is 200. The DFT/PCM calculations excludes any specific solvent molecules and thereby treat all of the solvent implicitly. Results are in eV.

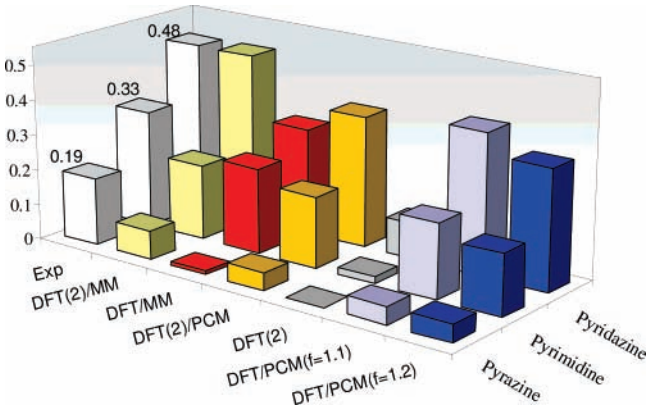

Figure 3. Calculated and experimental solvatochromic shifts (in eV) upon the n → π^* excitation. Experimental shifts (reported in the figure) are with respect to the isooctane solution.[13]

found with the effective cavities. The shifts, however, are still underestimated with respect to the experimental data, especially for pyrazine. A possible reason for this is that specific effects due to more than the two closest solvent molecules are important to include.

To check this, we can use the DPM. Treating only the solute molecule using DFT and all of the solvent molecules using MM (the DFT/MM results in Table 1 and in Figure 3) leads to results of comparable accuracy to the DFT(2)/PCM predictions. Treating again the two closest water molecules using DFT and the rest of the solvent using MM has only a minor effect on the shifts, except for pyridazine where a very good agreement with experimental data is obtained using such a scheme for solvation. As a further test, we have increased the closest water molecules treated using DFT passing from two to four; the results (shown in Table 1 only for pyrimidine) indicate that, in the case of the DPM, converged results are obtained by including only two water molecules into the DFT region (the two descriptions differ by only 0.01 eV).

A direct comparison with the results obtained with other discrete models is difficult due to both differences in the force fields and the level of the electronic structure theory used. For example, Almeida et al. obtained a solvent shift in the n → π^* electronic excitation in pyrimidine of 0.28 ± 0.01 eV based on Monte Carlo (MC) simulations combined with INDO/CIS calculations.[16] A similar result was also obtained by Gao et al. using MC simulations in combination with the AM1 Hamiltonian.[18] At the correlated level of theory, Martín et al. obtained 0.37 eV using the averaged solvent electrostatic potential (ASEP) combined with MD.[44]

From this first part of the analysis, DPM and PCM descriptions become close to each other (and to experiments) when PCM is modified so as to account explicitly or implicitly (i.e., using an effective cavity) for the specific effects of the hydrogen-bonded water molecules. The same specific effects alone, however, are not sufficient to properly describe the observed solvent effects.

A final comment on the results presented so far is that all solvent descriptions tend to underestimate the experimental solvent shifts. Several reasons may be attributed to these deviations between the experimental and theoretical results. Among them, we mention that we calculate the vertical electronic excitation energy and compare this to the peak of maximum absorption in the experimental spectra. Even though this is probably the most accurate way to compare calculated vertical electronic excitation energies to experiment, uncertainties in such a procedure may always exist. Furthermore, the results will depend on the quality of the force field used in the MD simulations to get the hydrogen-bonding clusters, and this may introduce additional errors in the calculation of the shifts (see section IV E for more details).

D. NMR Shielding Tensors. Having discussed the solvent effect on the lowest electronic excitation energies within the diazines, we next consider the NMR shielding constants. Here, we will focus on the nitrogen shielding constants. The results are presented in Table 2 and in Figure 4 for the absolute isotropic shieldings and the solvent-induced shifts, respectively.

Considering first the bare PCM with the standard cavity ($f = 1.2$), we find that solvent effects are underestimated as in the case of the excitation energies. The underestimation of the solvent shifts using PCM is again believed to be due to the neglect of specific interactions. As for the transition energies,

TABLE 2: The Nitrogen Isotropic NMR Chemical Shielding Constants (in ppm) in the Three Diazines in Vacuum and in Aqueous Solution[a]

method	pyrazine	pyrimidine	pyridazine
vacuum	−113.3	−72.1	−210.4
DFT/PCM ($f = 1.2$)	−101.8	−59.9	−176.1
DFT/PCM ($f = 1.1$)	−97.9	−55.7	−168.8
DFT(2)	−110.4 ± 0.8	−67.8 ± 0.5	−198.5 ± 1.0
DFT(2)/PCM	−99.7 ± 0.3	−57.4 ± 0.4	−171.0 ± 0.6
DFT/MM	−98.9 ± 0.8	−56.4 ± 0.5	−178.5 ± 1.0
DFT(2)/MM	−100.3 ± 0.8	−58.4 ± 0.5	−179.7 ± 1.0
DFT(4)/MM		−58.8 ± 0.5	

[a] The calculations have been performed using B3LYP/6-311++G(2d,2p), employing preoptimized geometries of the diazines computed at the B3LYP/aug-cc-pVTZ(/PCM) level of theory. The water potential used in the QM/MM calculations is the SPCpol. The number of solute−solvent configurations included in the averaging is 200. The DFT/PCM calculations exclude any specific solvent molecules.

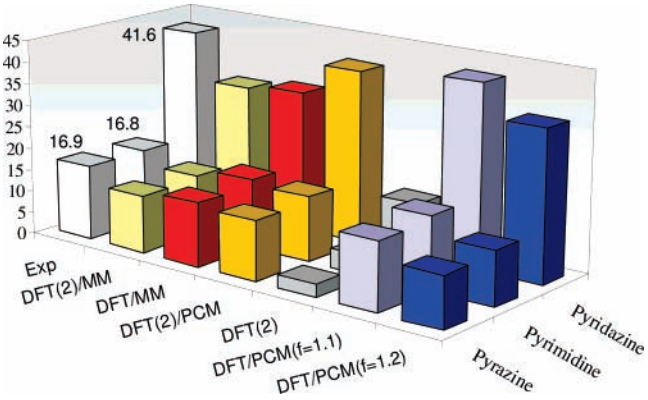

Figure 4. Calculated and experimental solvent-induced shifts (in ppm) on the nitrogen isotropic shielding. Experimental shifts (reported in the figure) are with respect to a cyclohexane solution.[46]

we can simulate these effects further by introducing an effective cavity (obtained with a scaling factor of $f = 1.1$). An increase of the shift is thus found for all molecules, leading to a better agreement with experimental data (especially for pyrimidine).

In contrast, the explicit consideration of the hydrogen-bonded water molecules using the DFT(2) approach, in which the two nearest water molecules are included in the system and the final results are averaged over 200 configurations, leads to extremely small shifts with respect to experiments (and also to the bare PCM).

Only by combining the two schemes (the DFT(2)/PCM entry in Table 2 and Figure 4) are very good results for the solvent shifts as compared to experimental data found. This shows that also for chemical shieldings, as for the transition energies, both specific and bulk effects are important. Once again, DFT(2)/PCM leads to a description quite similar to that obtained using only the PCM but with an effective cavity.

Moving to the results predicted using the DPM, we find that the DFT/MM model is able to provide results of comparable accuracy as those of the DFT(2)/PCM model (and DFT/PCM ($f = 1.1$)). This is not completely expected considering, for example, the results of a recent publication[42] where solvent effects on the NMR shielding constants of ^{17}O and ^{13}C clearly showed a marked difference between the PCM and MM descriptions of the solvent at least at the level of sophistication where no specific solvent molecules were treated quantum mechanically.

It must also be noted that small changes are generally observed when passing from completely classical water molecules (DFT/MM) to a description in which explicit water molecules are introduced into the region treated using DFT (DFT(2)/MM). Thus, we find the DPM model capable of providing almost converged results at the DFT/MM level where only the solute is treated using DFT.

TABLE 3: The Nonzero Components of the Reaction Field (E^{RF}) at the Nitrogen Nuclei in Pyrimidine Calculated Using Either DFT/MM or DFT/PCM Using, in Both Cases, B3LYP/6-311++G(2d,2p)[a]

method	site	E_y^{RF}	E_z^{RF}
DFT/MM	N1	−8.7 ± 0.4	7.3 ± 0.3
	N2	8.7 ± 0.4	7.3 ± 0.3
DFT/PCM (f=1.1)	N1	−7.6	8.6
	N2	7.6	8.6
DFT/PCM (f=1.2)	N1	−5.5	6.8
	N2	5.5	6.8
DFT/PCM (f=1.4)	N1	−2.9	4.3
	N2	2.9	4.3

[a] In these calculations, only the pyrimidine molecule is treated using DFT. The number of solute−solvent configurations included in the DFT/MM averaging is 200. The molecular coordinate system is defined according to Figure 5, that is, the pyrimidine molecule is confined to the yz plane, with the internal C_2 axis of pyrimidine along the z axis. Results are in 10^3 au.

In order to explore in more detail the similarities/differences between the PCM and DPM, we calculate the reaction field produced by either model at specific atomic sites. Both the PCM and DPM, in fact, produce an electric field at the solute, which perturbs the solute electronic density and thereby change the properties of the solute. In the case of PCM, the reaction field at site $\mathbf{R}_n$ is a true mean field produced by the ASC distribution represented by point charges, that is

$$\mathbf{E}^{RF}_{PCM}(\mathbf{R}_n) = \sum_{s=1}^{N} \frac{q_s^{PCM}(\mathbf{R}_n - \mathbf{R}_s)}{|\mathbf{R}_n - \mathbf{R}_s|^3} \tag{7}$$

On the other hand, for the DPM model, the reaction field is calculated by the expression

$$\mathbf{E}^{RF}_{DPM}(\mathbf{R}_n) = \sum_{s} \frac{q_s^{DPM}(\mathbf{R}_n - \mathbf{R}_s)}{|\mathbf{R}_n - \mathbf{R}_s|^3} + \sum_{a} \boldsymbol{\mu}_a^{ind} \mathbf{T}_{na} \tag{8}$$

where the first contribution in eq 8 is due to the point charges representing the permanent charge distribution of the solvent molecules and the second term represents the contribution from the induced dipoles at the polarizable sites in the solvent region. The symbol $\mathbf{T}$ is the dipole interaction tensor. The reaction field in eq 8 is calculated for each solute−solvent configuration, and thus, the DPM includes directly the fluctuations in the reaction field and the consequences this might have for the calculated properties.

In Table 3, we have shown the reaction field at the nitrogen sites of pyrimidine calculated using either DFT/MM or DFT/PCM. In case of DFT/MM, the results refer to averaging over 200 solute−solvent configurations. In the case of DFT/PCM, the reaction field has been calculated for different values of the cavity scaling factor. The coordinate system has been defined according to Figure 5, in which we show the geometry of the hydrogen-bonded system in a randomly chosen snapshot from the MD simulation of pyridine in water.

Within a given solvent model, the results for the reaction field are trivially related by symmetry (the N1 and N2 sites are, on average, indistinguishable). Due to the intrinsic differences between the PCM and DPM descriptions, the first provides

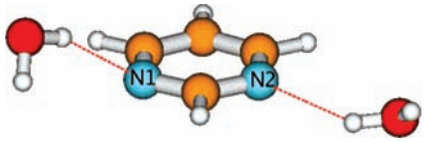

Figure 5. The atomic arrangement in a randomly chosen snapshot from the MD simulation of pyrimidine in water. Shown are only the two closest water molecules to each nitrogen site in pyrimidine. The pyrimidine molecule is confined to the *yz* plane with the internal C_2 axis of pyrimidine along the *z* axis.

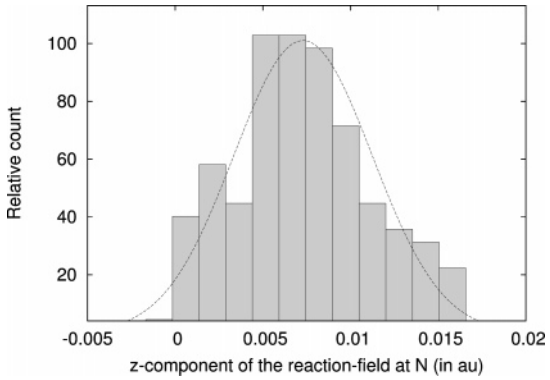

Figure 6. Statistical distribution for the *z* component (i.e., along the internal C_2 axis) of the reaction field of pyrimidine calculated using DFT/MM at the B3LYP/6-311++G(2d,2p) level. Only the pyrimidine molecule is treated using DFT. The number of solute−solvent configurations included in the DFT/MM averaging is 200. The electric field strength is in au.

only a number, whereas the latter gives a distribution of the reaction field. This distribution is shown in Figure 6 (the *z* component) and is seen to be quite broad, reflecting that different configurations give rise to quite different reaction fields.

As seen from Table 3, the PCM reaction field depends quite drastically on the cavity scaling factor. Choosing this to be equal to 1.4, which in the literature has been recommended in the case of less-polar solvents,[45] clearly underestimates the reaction field as compared to the DPM. This is also expected since water is to be considered as a high dielectric. Choosing the cavity scaling factor to be equal to 1.2 improves very much the results, but on average, a scaling factor of 1.1 gives the best results. We note, however, that it is not possible to obtain a common scaling factor that reproduces all of the DPM reaction-field components.

As shown in Figure 7a, an underestimation of the reaction field leads to an underestimation of the solvent shift in the ^{15}N NMR shielding constant. In fact, the relation between the reaction field and $\Delta\sigma^N$ is linear in this regime. Thereby, choosing the cavity scaling factor to be 1.1 results in an improved agreement between the DFT/MM and DFT/PCM results. In Figure 7b, we have also plotted the dependence on the PCM reaction field (*z* component) as a function of the cavity scaling factor. The reaction field is seen to exhibit a quadratic dependence on the cavity scaling factor.

The above analysis may provide some information on the differences/similarities in the physics within the PCM and DPM models. Since the bare radius of the nitrogen atom is ∼1.5 Å, the solvent will, in the case of the PCM, be placed either 1.65 ($f = 1.1$) or 1.80 ($f = 1.2$) Å away from the nitrogen site. In contrast, in the MD simulations and therefore also in the DPM calculations, the solvent is, on average, placed 1.96 Å from the nitrogen site, as inferred from the nitrogen−hydrogen RDF in pyrimidine. Furthermore, the oxygen site of water will be placed, on average, around 0.96 Å (approximately the OH bond length in water) even further from the nitrogen site. This is important since the hydrogen site in water is much less polarizable than the oxygen site. This mean that, on average, the solvent is placed (much) further away from the solute within the DPM as compared to in the PCM. Choosing the cavity dimensions so as to reproduce the structural data from the MD simulation would, according to Figure 7, lead to very underestimated results for the solvent shifts in the NMR shielding constants as compared to either the DPM or to experimental data. Thereby, the bare PCM properly works by effectively placing the solvent closer to the solute as compared to MD data, which leads to an overall good agreement between the predicted and experimental data.

In order to explore the solvent shifts on the nitrogen NMR shielding constants obtained with the two solvent models in more detail, we consider in Table 4 the three components of the NMR shielding tensor determining the isotropic values. The results presented in Table 4 are absolute NMR shielding constants.

In the PCM, we have used three different cavity scaling factors ($f = 1.1$, 1.2, or 1.4). From the first three entries in Table 4, we observe that changing the cavity scaling factor has a quite different outcome for the three diagonal components of the NMR shielding tensor. The *xx* component (out of plane) is almost unchanged, whereas the magnitudes of the *yy* or *zz* components increases around 10 or 20 ppm, respectively, by changing the cavity scaling factor from 1.1 to 1.4. Thereby, we observe a span in the tensor components which is larger than the span in the isotropic values. As already observed for the isotropic value (and further confirmed for the reaction field in Table 3), we find that using $f = 1.1$ gives the best results for the shielding components as compared to DFT/MM. If we also introduce two explicitly treated water molecules (the DFT(2)/PCM entry), the agreement becomes even closer. Turning to the DPM results, we find here that introducing two water molecules into the DFT-treated region leads to an average change in each tensor component of around 1.9 ppm. More evident than that with PCM, the origin of this change is found to be almost entirely due to changes in the *zz* component (along the C_2 axis in pyrimidine). Thus, within the DPM model, a faster convergence is observed with respect to the number of solvent molecules treated using DFT for both the isotropic value and diagonal components of the NMR shielding tensor.

Defining the DFT(2)/MM results in Table 4 as the reference, Figure 8 displays the deviation between the tensor components and the isotropic NMR shielding between the various models and the reference. From Figure 8, it is evident that for both the isotropic and each tensor component, the DFT(2)/MM results are better reproduced by DFT(2)/PCM than by DFT/MM. This clearly illustrates that special (QM) treatment of the solvent molecules very close to the solute may be important, whereas the bulk solvent is described equally well using either a PCM or a DPM. It is also interesting to observe that a good agreement is found instead between DFT/PCM($f = 1.1$) and DFT/MM. Such an agreement might be related to the fact that both models introduce "artificial" short-range solute−solvent interactions (one in terms of a smaller cavity and the other in terms of purely classical dipoles), while an important part of these interactions (charge-transfer, dispersion, and other QM effects) is not taken into account.

E. Comparison with Geometry-Optimized Solute−Solvent Clusters. As an alternative approach to account for solvation, we finally consider the case where the solute and a few (in this case two) explicit solvent molecules are geometry-optimized

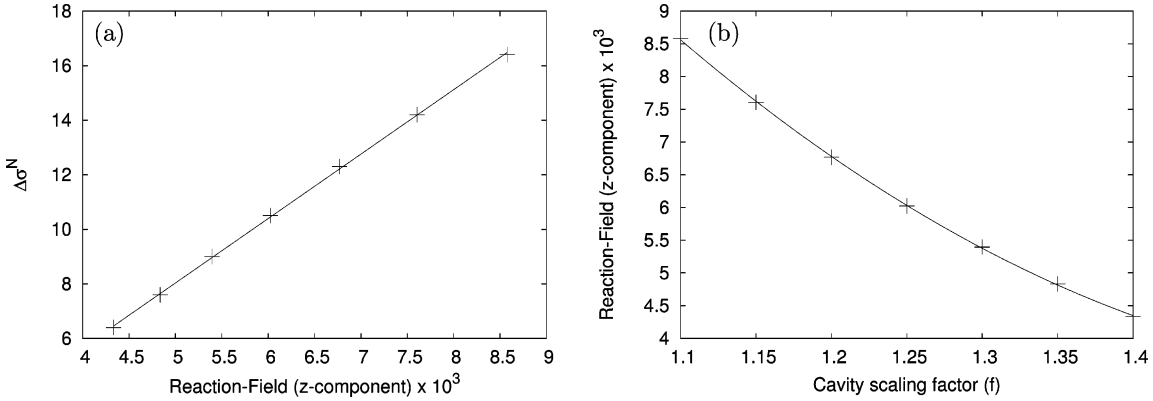

Figure 7. The dependence on (a) the solvation shift of the nitrogen isotropic NMR shielding constant of pyrimidine with respect to the *z* component of the reaction field, RFz, and (b) the *z* component of the reaction field with respect to the cavity scaling factor, *f*. All calculations refer to DFT/PCM at the B3LYP/6-311++G(2d,2p) level of theory. The molecular coordinate system is defined according to Figure 5. Included in the PCM is only the pyrimidine molecule. Shown are the data points together with fitted lines, that is, (a) $\Delta\sigma^N = 2.36 \times 10^3 \mathrm{RFz} - 3.78$ and (b) $\mathrm{RFz}(\times 10^3) = 18.8f^2 - 61.04f + 52.95$.

TABLE 4: The Diagonal Tensor Elements as Well as the Isotropic Value of the Absolute NMR Shieldings for Pyrimidine Calculated Using Various Solvent Models[a]

method	σ^N_{xx}	σ^N_{yy}	σ^N_{zz}	$\bar{\sigma}^N$
DFT/PCM ($f = 1.1$)	275.9	−212.2	−230.7	−55.7
DFT/PCM ($f = 1.2$)	275.5	−216.1	−239.0	−59.9
DFT/PCM ($f = 1.4$)	275.3	−221.8	−250.6	−65.7
DFT(2)/PCM	274.2 ± 0.2	−211.3 ± 0.7	−235.1 ± 1.4	−57.4 ± 0.4
DFT/MM	273.6 ± 0.2	−211.5 ± 0.7	−231.3 ± 1.4	−56.4 ± 0.5
DFT(2)/MM	273.2 ± 0.2	−212.0 ± 0.7	−236.3± 1.4	−58.4 ± 0.5

[a] The molecular coordinate system is defined according to Figure 5. All results are in ppm.

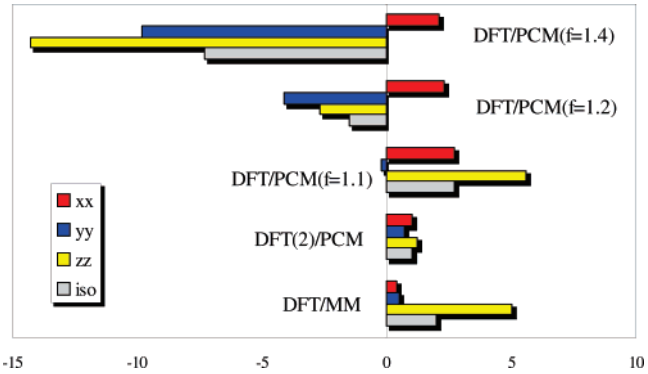

Figure 8. Deviation between the diagonal ^{15}N NMR shielding tensor components as well as the mean isotropic value calculated using various solvation models with respect to the DFT(2)/MM numbers (ref model). The data are compiled from Table 4. The cavity radius used in the PCM-only calculations are given in parenthesis. The results are in ppm.

in the presence of the PCM. Here, we use B3LYP/aug-cc-pVTZ/PCM for the geometry optimizations, while the property calculations have been performed using B3LYP/6-311++G-(2d,2p)/PCM. In all cases, we use the default cavity scaling factor of 1.2.

The results based on the geometry-optimized clusters are shown in Table 5. In contrast to the MD results, the hydrogen bond between the nitrogen site of the solute and the hydrogen of water has, in the geometry-optimized solute−solvent clusters approximately, the same length for all three solutes. This hydrogen bond distance, $R(\mathrm{N}\cdots\mathrm{H}) = 1.92$ Å, is in addition shorter than any of the corresponding hydrogen bonds (on average) predicted from the MD simulations. This is not

TABLE 5: The Nitrogen Isotropic NMR Chemical Shielding Constants (in ppm), σ^N, the Solvent Shift Due to Water, $\Delta\sigma^N$, the Lowest Electronic Excitation Energy (eV), $\Delta E(\mathrm{n} \rightarrow \pi^*)$, as Well as the Solvent Shift Due to Water for the Three Diazines[a]

	pyrazine	pyrimidine	pyridazine
$\Delta E(\mathrm{n} \rightarrow \pi^*)$	4.11	4.59	4.10
shift (PCM)	0.16	0.31	0.55
shift (exptl)	0.19	0.33	0.48
σ^N	−92.5	−51.9	−152.2
$\Delta\sigma^N$ (PCM)	20.8	20.2	59.2
$\Delta\sigma^N$ (exptl)	16.9	16.8	41.6

[a] The results have been obtained from geometry optimizations of each diazine, including two explicit water molecules together with the PCM. The geometry optimizations have been obtained using B3LYP/aug-cc-pVTZ/PCM, and the property calculations have been performed using B3LYP/6-311++G(2d,2p)/PCM.

surprising since the outcome from the geometry optimizations are equilibrium structures at $T = 0$ K, representing the lowest energies on the potential energy surfaces, which physically might be very different from the true liquid at finite temperatures.

Due to the shorter hydrogen bond distances, we observe, as compared to the MD-derived results, an increase in the effect of solvation for all properties. Such an increased effect of solvation for geometry-optimized clusters as compared to simulation-based results have also been found in other studies; see, for example, the work by Canuto et al. on binding energies for the related pyridine compound in water solution.[43] In the present study, the solvent-induced shift on the excitation energies actually compares better with the experimental data (Figure 3) than that in the case of the statistically based methods. However, the use of geometry-optimized clusters may also lead to overestimated solvent effects (for pyridazine). Turning to the NMR parameters, the situation is different. In this case, the MD-based results were found to compare reasonably well with the experimental data (Figure 4). However, as for the electronic excitation energies, the use of geometry-optimized clusters leads to enhanced solvent effects and, in this case, to consistently overestimated shifts. For pyridazine, this overestimation amounts to around 17 ppm or around 40% of the experimentally determined solvent shift. Thereby, we find no coherent picture from the use of geometry-optimized clusters as compared to experimental data. On the other hand, within the PCM or dynamical approaches, the solvent effects are almost always underestimated as compared to experimental data. This indicates that improvement within the dynamical scheme could be

obtained by considering hydrogen bonding explicitly in the force field, for example, a reparameterization of the diazine force field taking explicitly into account the effect of the lone pairs on the nitrogen sites in order to improve the hydrogen bond formation. This would probably lead to an enhanced stability (solvation) of the electronic ground state, as observed for the geometry-optimized clusters, and thereby to an increase in the solvent effects on the electronic excitation energies. For the NMR parameters, the analysis is more complicated since these properties implicitly depend on the manifold of all electronic states and not just the ground and a specific excited state. as in the case of the electronic excitation energies. However, on the basis of the results from the geometry-optimized clusters, the previous-described reparameterization of the force field is expected also to lead to enhanced solvent shifts on the NMR parameters.

V. Summary

In this paper, we have presented a comparative study on the performances of continuum (PCM) and discrete (DPM) polarizable solvation models when describing solvent effects on excitation energies and NMR parameters. In particular, the attention has been focused on the three diazines in water, that is, a solvent which can act as a hydrogen-bond donor with respect to the diazine nitrogen atoms.

The results have been analyzed directly in terms of the solvent-induced shifts with respect to experimental data and indirectly in terms of the reaction field produced by either the PCM or the DPM. The reaction field produced by the PCM is found to depend very much on the dimension of the cavity. Choosing scaling factors for the cavity of 1.1 reproduces quite well the DPM reaction field. In addition, if this value of the cavity scaling factor is used, the excitation energies as well as the isotropic and anisotropic NMR shielding constants agree well between the PCM and the DPM. As compared to experimental data, we find that the most accurate results are obtained by including a few solvent molecules into the region treated using DFT. This allows for explicit treatment of intermolecular charge-transfer, short-range, and improved electrostatic effects. Also, part of the intermolecular interactions related to dispersion is included. The bulk solvent may, on the other hand, be described by an effective approach where either the PCM or the DPM may be used. However, we emphasize that it is mandatory to include contributions from both the nearby and bulk solvent. On the basis of either the dynamical or PCM approaches, the solvent effects on both the UV and NMR properties tend to be underestimated. On the other hand, results based on small geometry-optimized clusters (including the PCM for the bulk solvent) tend to be overestimated especially for the NMR properties. As mentioned previously, in all calculations, we have neglected rovibrational averaging, which may be important for accurate evaluation of the solvent-induced shifts and represent a potential source of uncertainty; however, it seems that checks on possible deficiencies in the underlying force field used in the MD simulations are always necessary in order to accurately describe the effect of hydrogen bonding.

Acknowledgment. J.K. acknowledges support from the Villum Kann Rasmussen Foundation (Denmark). The authors thank Professor Kenneth Ruud, University of Tromsø, Norway, for useful discussions.

References and Notes

(1) Helgaker, T.; Jørgensen, P.; Olsen, J. *Molecular Electronic Structure Theory*; Wiley: New York, 2000.

(2) (a) Canuto, S.; Coutinho, K. *Int. J. Quantum Chem.* **2000**, *77*, 192. (b) Canuto, S.; Coutinho, K. *J. Chem. Phys.* **2000**, *113*, 9132.

(3) Aidas, K.; Kongsted, J.; Osted, A.; Mikkelsen, K. V.; Christiansen, O. *J. Phys. Chem. A* **2005**, *109*, 8001.

(4) Coriani, S.; Høst, S.; Jansik, B.; Thøgersen, L.; Olsen, J.; Jørgensen, P.; Reine, S.; Pawlowski, F.; Helgaker, T.; Salek, P. *J. Chem. Phys.* **2007**, *126*, 154108.

(5) Tomasi, J.; Mennucci, B.; Cammi, R. *Chem. Rev.* **2005**, *105*, 2999.

(6) Warshel, A.; Levitt, M. *J. Mol. Biol.* **1976**, *103*, 227.

(7) Singh, U. C.; Kollman, P. A. *J. Comput. Chem.* **1986**, *7*, 718.

(8) Field, M. J.; Bash, P. A.; Karplus, M. *J. Comput. Chem.* **1990**, *11*, 700.

(9) Thompson, M. A. *J. Phys. Chem.* **1996**, *100*, 14492.

(10) Kongsted, J.; Osted, A.; Mikkelsen, K. V.; Christiansen, O. *Mol. Phys.* **2002**, *100*, 1813.

(11) Nielsen, C. B.; Christiansen, O.; Mikkelsen, K. V.; Kongsted, J. *J. Chem. Phys.* **2007**, *126*, 154112.

(12) Becke, A. D. *J. Chem. Phys.* **1993**, *98*, 5648.

(13) Baba, H.; Goodman, L.; Valenti, P. C. *J. Am. Chem. Soc.* **1966**, *88*, 5410.

(14) Brealey, G. J.; Kasha, M. *J. Am. Chem. Soc.* **1955**, *77*, 4462.

(15) Krishna, V. G.; Goodman, L. *J. Am. Chem. Soc.* **1961**, *83*, 2042.

(16) de Almeida, K. J.; Coutinho, K.; de Almeida, W. B.; Rocha, W. R.; Canuto, S. *Phys. Chem. Chem. Phys.* **2001**, *3*, 1583.

(17) Karelson, M. M.; Zerner, M. C. *J. Phys. Chem.* **1992**, *96*, 6949.

(18) Gao, J.; Byun, K. *Theor. Chem. Acc.* **1997**, *96*, 151.

(19) (a) Zeng, J.; Hush, N. S.; Reimers, J. *J. Chem. Phys.* **1993**, *99*, 1482. (b) Zeng, J.; Hush, N. S.; Reimers, J. *J. Chem. Phys.* **1993**, *99*, 1496. (c) Zeng, J.; Hush, N. S.; Reimers, J. *J. Chem. Phys.* **1993**, *99*, 1508. (d) Zeng, J.; Hush, N. S.; Reimers, J. *J. Phys. Chem.* **1996**, *100*, 9561.

(20) Mennucci, B. *J. Am. Chem. Soc.* **2002**, *124*, 1506.

(21) Tomasi, J.; Persico, M. *Chem. Rev.* **1994**, *94*, 2027.

(22) (a) Cancés, E.; Mennucci, B.; Tomasi, J. *J. Chem. Phys.* **1997**, *107*, 3031. (b) Mennucci, B.; Cancés, E.; Tomasi, J. *J. Phys. Chem. B* **1997**, *101*, 10506.

(23) Osted, A.; Kongsted, J.; Mikkelsen, K. V.; Christiansen, O. *Mol. Phys.* **2003**, *101*, 2055.

(24) Salek, P.; Vahtras, O.; Helgaker, T.; Ågren, H. *J. Chem. Phys.* **2002**, *117*, 9630.

(25) Cammi, R.; Frediani, L.; Mennucci, B.; Ruud, K. *J. Chem. Phys.* **2003**, *119*, 5818.

(26) Olsen, J.; Jørgensen, P. *J. Chem. Phys.* **1985**, *82*, 3235.

(27) Helgaker, T.; Jaszunski, M.; Ruud, K. *Chem. Rev.* **1999**, *99*, 293.

(28) London, F. *J. Phys. Radium* **1937**, *8*, 397.

(29) (a) Hameka, H. F. *Rev. Mod. Phys.* **1962**, *34*, 87. (b) Ditchfield, R. *Mol. Phys.* **1974**, *27*, 789. (c) Wolinski, K.; Hinton, J. F.; Pulay, P. *J. Am. Chem. Soc.* **1990**, *112*, 8251.

(30) Cammi, R.; Mennucci, B.; Tomasi, J. *J. Chem. Phys.* **1999**, *110*, 7627.

(31) Pecul, M.; Marchesan, D.; Ruud, K.; Coriani, S. *J. Chem. Phys.* **2005**, *122*, 024106.

(32) Kongsted, J.; Nielsen, C. B.; Mikkelsen, K. V.; Christiansen, O.; Ruud, K. *J. Chem. Phys.* **2007**, *126*, 034510.

(33) Molsim is an integrated md/mc/bd simulation program belonging to the molsim package. Linse, P. *Molsim*, version 3.3.0; Lund University: Sweden, Dec 05, 2001.

(34) Jorgensen, W. L.; McDonald, N. A. *J. Mol. Struct.: THEOCHEM* **1998**, *424*, 145.

(35) Frisch, M. J.; Trucks, G. W.; Schlegel, H. B.; Scuseria, G. E.; Robb, M. A.; Cheeseman, J. R.; Montgomery, J. A., Jr.; Vreven, T.; Kudin, K. N.; Burant, J. C.; Millam, J. M.; Iyengar, S. S.; Tomasi, J.; Barone, V.; Mennucci, B.; Cossi, M.; Scalmani, G.; Rega, N.; Petersson, G. A.; Nakatsuji, H.; Hada, M.; Ehara, M.; Toyota, K.; Fukuda, R.; Hasegawa, J.; Ishida, M.; Nakajima, T.; Honda, Y.; Kitao, O.; Nakai, H.; Klene, M.; Li, X.; Knox, J. E.; Hratchian, H. P.; Cross, J. B.; Bakken, V.; Adamo, C.; Jaramillo, J.; Gomperts, R.; Stratmann, R. E.; Yazyev, O.; Austin, A. J.; Cammi, R.; Pomelli, C.; Ochterski, J. W.; Ayala, P. Y.; Morokuma, K.; Voth, G. A.; Salvador, P.; Dannenberg, J. J.; Zakrzewski, V. G.; Dapprich, S.; Daniels, A. D.; Strain, M. C.; Farkas, O.; Malick, D. K.; Rabuck, A. D.; Raghavachari, K.; Foresman, J. B.; Ortiz, J. V.; Cui, Q.; Baboul, A. G.; Clifford, S.; Cioslowski, J.; Stefanov, B. B.; Liu, G.; Liashenko, A.; Piskorz, P.; Komaromi, I.; Martin, R. L.; Fox, D. J.; Keith, T.; Al-Laham, M. A.; Peng, C. Y.; Nanayakkara, A.; Challacombe, M.; Gill, P. M. W.; Johnson, B.; Chen, W.; Wong, M. W.; Gonzalez, C.; Pople, J. A. *Gaussian 03*, revision B.05; Gaussian, Inc.: Wallingford, CT, 2004.

(36) Ahlström, P.; Wallqvist, A.; Engström, S.; Jönsson, B. *Mol. Phys.* **1989**, *68*, 563.

(37) *Dalton, a Molecular Electronic Structure Program*, release 2.0; 2005; see http://www.kjemi.uio.no/software/dalton/dalton.html.

(38) Christiansen, O. *Midascpp, Molecular Interactions, Dynamics and Simulation in C++*; University of Aarhus, 2004.

(39) Kendall, R. A.; Dunning, T. H.; Harrison, R. J. *J. Chem. Phys.* **1992**, *96*, 6796.

(40) Frisch, M. J.; Pople, J. A.; Binkley, J. S. *J. Chem. Phys.* **1984**, *80*, 3265.

(41) Cossi, M.; Crescenzi, O. *J. Chem. Phys.* **2003**, *118*, 8863.

(42) Aidas, K.; Møgelhøj, A.; Kjær, H.; Nielsen, C. B.; Mikkelsen, K. V.; Ruud, K.; Christiansen, O.; Kongsted, J. *J. Phys. Chem. A* **2007**, *111*, 4199.

(43) Malaspina, T.; Coutinho, K.; Canuto, S. *J. Chem. Phys.* **2002**, *117*, 1692.

(44) Martín, M. E.; Sánchez, M. L.; Aguilar, M. A.; del Valle, F. J. O. *J. Mol. Struct.*: *THEOCHEM* **2001**, *537*, 213.

(45) (a) Luque, F. J.; Bachs, M.; Aleman, C.; Orozco, M. *J. Comput. Chem.* **1996,** *17*, 806. (b) Cossi, M.; Crescenzi, O. *Theor. Chem. Acc.* **2004**, *111*, 162.

(46) Witanowski, M.; Stefaniak, L.; Webb, G. A. *Annual Reports on NMR Spectroscopy*; Academic Press: London, 1993; Vol. 25.